Materials Science-Poland, Vol. 27, No. 2, 2009

Electrical properties of tin phthalocyanine-based heterostructures: $SnPcCl_2$/GaP, $SnPcCl_2$/InP and $SnPcCl_2$/GaAs

M.M. EL-NAHASS[1], A.M. FARID[1], H.H. AMER[2], K.F. ABDEL-RAHMAN[1*], H.A.M. ALI[1]

[1]Faculty of Education, Ain Shams University, Cairo, Egypt

[2]National Centre for Radiation Research and Technology, Nasr City, Cairo, Egypt

Electrical characteristics of organic/inorganic, $SnPcCl_2$/GaP, $SnPcCl_2$/GaAs and $SnPcCl_2$/InP (Pc standing for phthalocyanine) heterojunctions were studied. Current density–voltage (*J–V*) characteristics showed thermionic emission conduction at relatively low voltages followed by a space charge limited conduction mechanism at relatively high voltages. The capacitance–voltage (*C–V*) characteristics indicated that the devices have an abrupt nature. Various parameters have been determined from the *J–V* and *C–V* analysis for the three devices.

Key words: *phthalocyanines; organic/inorganic heterojunction*

1. Introduction

A considerable interest in electrical and optical properties of organic molecular semiconductors reflects their increasingly widespread use in organic and hybrid organic-inorganic (OI) devices [1]. When organic semiconductors are deposited onto inorganic semiconductor substrates such as Si or InP, a rectifying energy barrier is formed at the OI interface [2]. Transport of charge across the energy barrier is limited by various mechanisms.

Organic semiconductors like phthalocyanines have been intensively studied with regard to their electrical and photoconduction properties [3]. Phthalocyanines are generally p-type semiconductors and have the advantage of being sufficiently stable under chemical and thermal treatment. They can be easily vacuum deposited, find application in gas sensors and various organic optoelectronic devices such as solar cells, light-emitting diodes as hole transport layers [6–9] in high purity thin films without

*Corresponding author, e-mail: elrahman99@hotmail.com

decomposition [4, 5]. Electronic devices with phthalocyanines as the active materials can be fabricated on a wide variety of substrates [5]. Phthalocyanines have attracted a lot of attention in view of their possible applications in organic-inorganic structures. They are expected to open up new areas of research in optoelectronic materials, because they make it possible to include and exploit in a single system the specific light absorption characteristics of the organic molecules as well as the good carrier mobility of the inorganic materials [10, 11]. Recently, efforts have been exerted to combine the desired properties of inorganic and organic layers in optoelectronic junctions. Takada et al. [12] have demonstrated an example of the formation of CuPc/TiO heterostructure; these junctions were found to exhibit 40 times higher photoconductivity than a single layer of CuPc. Recently, Lee et al. [13] have fabricated PbTe/CuPc heterojunctions.

Among various phthalocyanines, tin phthalocyanine dichloride ($SnPcCl_2$) has received less attention than others. The object of this paper is to investigate the electrical characteristics of $SnPcCl_2$/GaP, $SnPcCl_2$/GaAs and $SnPcCl_2$/InP heterojunctions. In particular, the voltage properties of the different substrates were investigated in a controlled-light environment, in order to test the response of the heterojunctions to illumination and to total darkness. Also, capacitance-voltage measurements were carried out in the dark in order to characterize these cells.

2. Experimental

The films were fabricated using tin phthalocyanine dichloride ($SnPcCl_2$) which had been purchased from the ACROS Organics Company, USA. Gallium phosphide (GaP), gallium arsenide (GaAs) and indium phosphide (InP) single crystals were used as substrates in order to fabricate different organic/inorganic diodes. The substrates were cleaned and etched before the device fabrication. The substrates were rinsed in distilled water, ethyl alcohol and acetone for 2 min, and then in distilled water for 1 min. The substrates were then etched for 45 s in aqueous solution of H_2O_2 and H_2SO_4. After etching, the substrates were washed for 1 min in distilled water and then dried with nitrogen. All surface treatments were chosen such that they would not attack the underlying semiconductor but would rather only affect the surface region.

After surface cleaning, the samples were mounted inside the vacuum chamber of an Edward 306 evaporator unit. A thin film of $SnPcCl_2$ with a thickness of 325 nm was then deposited onto the clean surface of the substrates by thermal evaporation. The evaporation was carried out by sublimation of the $SnPcCl_2$ powder from a quartz crucible source heated with a tungsten coil in the vacuum of 10^{-4} Pa with the deposition rate of 2.5 $nm \cdot s^{-1}$. The substrate temperature was kept at 300 K during the deposition. The OI devices were completed by vacuum deposition of an ohmic Au contact using a suitable mask placed in contact with the top of the $SnPcCl_2$ layer. The other ohmic contact was made to the back wafer surface, also by vacuum deposition of Ag. A typical heterojunction is shown in Fig. 1a.

In the present paper, the electrical characteristics of $SnPcCl_2$/GaP, $SnPcCl_2$/GaAs and $SnPcCl_2$/InP hetrerojunctions were examined by using current density–voltage (*J–V*) measurements in the dark. The current flowing through the device was determined using a stabilized power supply and a high impedance electrometer (Keithley 617 A).

Also, capacitance–voltage (*C–V*) measurements were performed at a frequency of 1 MHz using a computerized (*C–V*) system, consisting of a 410 *C–V* meter, controlled via interface with a 4108 *C–V* connected to a personal computer.

3. Results and discussion

3.1. Dark *J–V* characteristics

J–V characteristics at room temperature for the three fabricated diodes structures; Au/$SnPcCl_2$/GaP/Ag, Au/$SnPcCl_2$/GaAs/Ag and Au/$SnPcCl_2$/InP/Ag, are shown in Fig. 1b. The differences in the behaviour of these devices result from a significant difference between the inorganic substrates and the nature of the OI interface. The rectification ratio for Au/$SnPcCl_2$/GaP/Ag at 1.4 V was found to be about 100 and this value was higher than those obtained for the other diodes.

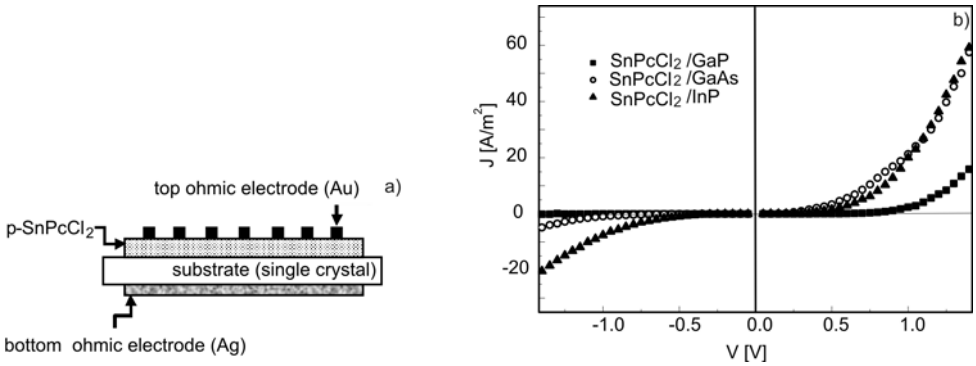

Fig. 1. Typical schematic diagram of p-$SnPcCl_2$/n-substrate (GaP or GaAs or InP), heterojunction (a), and *I–V* characteristics at room temperature for p-$SnPcCl_2$/n-GaP, p-$SnPcCl_2$/n-GaAs and p-$SnPcCl_2$/n-InP contact barrier diodes

J–V characteristics for various heterojunction devices under a forward bias at several temperatures ranging from 293 to 373 K are shown in Fig. 2. As observed from the figure, the current density increases exponentially with the applied voltage and then deviates from the exponential due to the effect of series resistance on the system. So, the forward current can be classified into two regions according to the applied voltage. In the first region (low voltage, $V < 0.5$ V), the *J–V* characteristics of the de-

vices follow the dependence characteristic of thermionic emission theory for conduction across the junction, which can be expressed by the following equation [14]

$$J = J_s \exp\left(\frac{qV}{nk_BT}\right) - 1 \tag{1}$$

where J_s is the reverse saturation current density, q is the electronic charge, n is the diode quality factor, which accounted for the extent of the non-ideality of the diode and k_B is the Boltzmann constant.

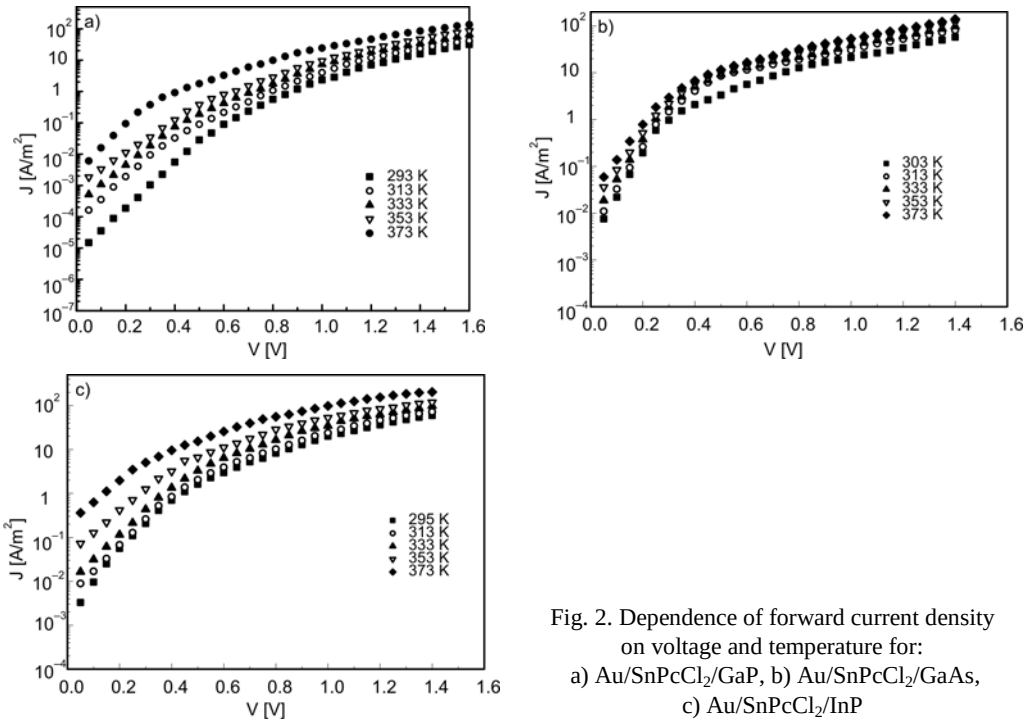

Fig. 2. Dependence of forward current density on voltage and temperature for: a) Au/SnPcCl$_2$/GaP, b) Au/SnPcCl$_2$/GaAs, c) Au/SnPcCl$_2$/InP

The saturation current density, J_s, is given by [14]:

$$J_s = A^* T^2 \exp\left(-\frac{\phi_B}{k_BT}\right) \tag{2}$$

where A^* is the effective Richardson constant, and ϕ_B is the Schottky barrier height of the diode. Applying this theory, the values of the diode quality factor n and the reverse saturation current density J_s have been calculated and collected in Table 1. The value of n is greater than unity which can be attributed to the recombination of the electrons and holes in the depletion region [15]. The potential barrier ϕ_B has been calculated by employing the same theory and is compiled in Table 1. It is observed that the Schottky

barrier effect disappears when the applied voltage is 0.63, 0.58 and 0.26 V in $SnPcCl_2$/GaP, $SnPcCl_2$/InP and $SnPcCl_2$/GaAs devices, respectively. Beyond these, the current density is mainly contributed from the bulk resistance of $SnPcCl_2$ layer. The $SnPcCl_2$/GaAs and $SnPcCl_2$/InP devices exhibit smaller contact barrier heights than that obtained for the $SnPcCl_2$/GaP heterojunction device, as seen from Table 1. The relatively small OI barrier heights are found to arise from a high density of states at the inorganic substrate surface [16].

Table 1. Electrical parameters derived from the analysis of *J–V* characteristics

Sample	n	J_s [A/m^2]	ϕ_B [eV]
Au/$SnPcCl_2$/GaP/Ag	2.34	7.476×10^{-6}	0.63
Au/$SnPcCl_2$/InP/Ag	2.75	7.895×10^{-4}	0.58
Au/$SnPcCl_2$/GaAs/Ag	1.81	2.5×10^{-3}	0.26

In the second region (relatively high voltage, $V > 0.5$ V), the conduction may be attributed to the space charge limited currents in the organic layer. It is observed that the current density shows a power dependence of voltage of the type $J \propto V^m$ for the three devices as seen in Fig. 3. The calculated value of m is higher than 2, as seen in Table 2, thus this power dependence shows that the forward biased current is a space charge limited current (SCLC) dominated by an exponential distribution of traps.

Table 2. The parameters derived from the *J–V* analysis in the SCLC region

Parameter	$SnPcCl_2$/GaP	$SnPcCl_2$/GaAs	$SnPcCl_2$/InP
m	6.24	2.6	3.14
T_t [K]	1538	485	631.3
μ, [m^2·s^{-1}·V^{-1}]	8.19×10^{-9}	4.35×10^{-12}	3.53×10^{-11}
N_t [m^{-3}]	1.75×10^{21}	1.85×10^{21}	2.28×10^{21}
P_0 [J^{-1}·m^{-3}]	8.26×10^{40}	2.76×10^{41}	2.61×10^{41}
E_r [eV]	0.34	0.29	0.23

The current density in this region is given by [16]:

$$J = q\mu N_V \left(\frac{\varepsilon}{eP_0 k_B T_t} \right)^l \frac{V^{l+1}}{d^{2l+1}} \tag{3}$$

where μ is the hole mobility, N_V is the effective density of states at the valence band edge, taken as 10^{27} m^{-3} [17], ε is the permittivity of the $SnPcCl_2$ taken as 3.214×10^{-11} F·m^{-1} [18], P_0 is the trap concentration per unit energy range at the valence band edge, l is the ratio between the temperature parameter T_t and the ambient temperature. The pa-

rameter T_t is the characteristic temperature of the exponential trap distribution, tabulated in Table 2 for the three junctions. The total concentration of traps is given by:

$$N_t = P_0 k_B T_t \tag{4}$$

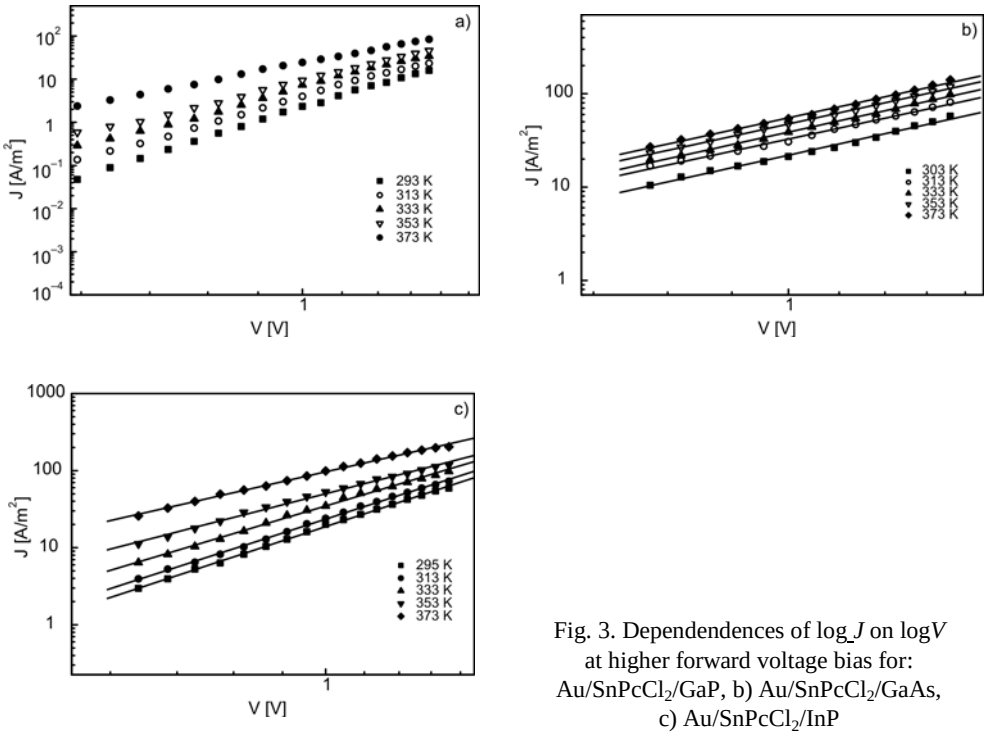

Fig. 3. Dependences of log$J$ on log$V$ at higher forward voltage bias for: Au/$SnPcCl_2$/GaP, b) Au/$SnPcCl_2$/GaAs, c) Au/$SnPcCl_2$/InP

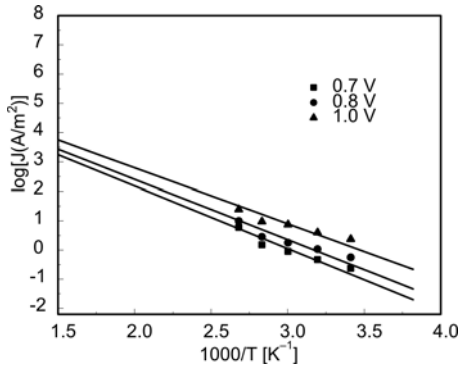

Fig. 4. Dependences of log$J$ on 1000/T in SCLC for $SnPcCl_2$/GaP device

The value of N_t can be obtained from the variation of the current density with the temperature in the SCLC region. As shown in Fig. 4, the dependences of log$J$ on 1000/T for the $SnPcCl_2$/GaP heterojunction are straight lines. The same behaviour was also obtained for the other two devices. The slope of these lines is given by [17, 19]:

$$\frac{d\left(\log J\right)}{d\left(\frac{1}{T}\right)} = T_t \log \frac{\varepsilon V}{ed^2 N_t} \tag{5}$$

The value of μ, has been calculated from the intercept of the line in Fig. 4 given by [5]:

$$\log J_0 = \log \frac{q\mu N_V V}{d} \tag{6}$$

The values of μ, N_t and P_0 have been calculated for the three heterojunctions (Table 2). The electrical parameters derived from the *J–V* analysis in the SCLC region, are consistent with the values reported for some other metal phthalocyanines (MPc's).

The measured reverse-bias characteristics of SnPcCl$_2$/GaP, SnPcCl$_2$/GaAs and SnPcCl$_2$/InP heterojunctions at various temperatures are shown in Fig. 5. A relatively bias dependence of the reverse current is observed which could be due to the recharging of trapping states within the junction region [20].

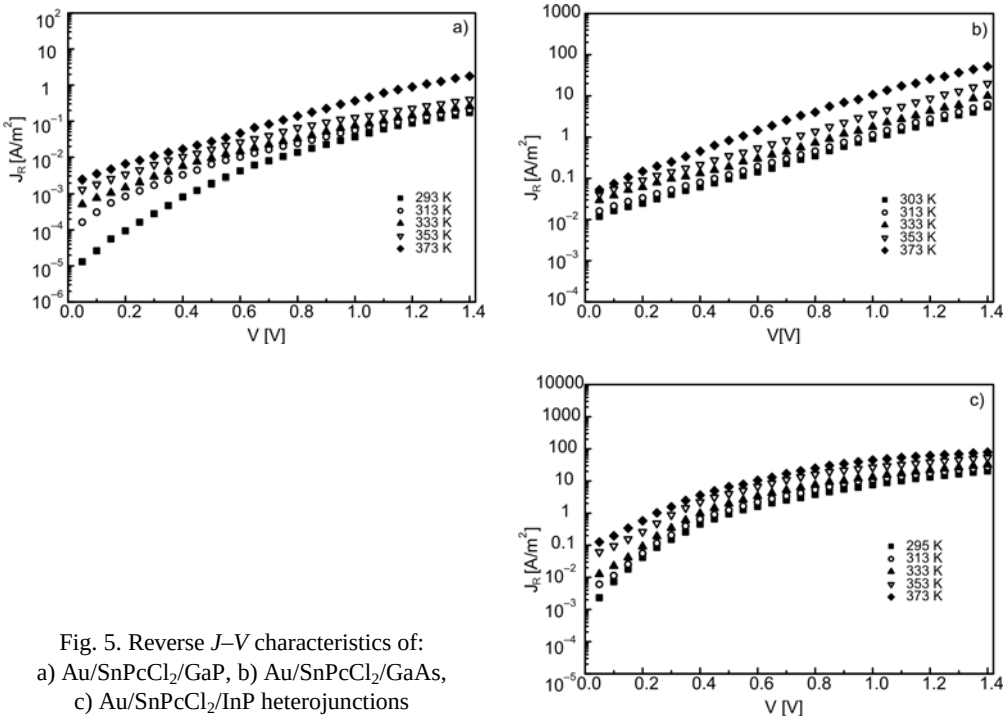

Fig. 5. Reverse *J–V* characteristics of:
a) Au/SnPcCl$_2$/GaP, b) Au/SnPcCl$_2$/GaAs,
c) Au/SnPcCl$_2$/InP heterojunctions

Figure 6 shows the temperature dependences of the reverse current of SnPcCl$_2$/GaP, SnPcCl$_2$/GaAs and SnPcCl$_2$/InP heterojunctions. ln(J_R) was plotted in function of 1000/T at various reverse-bias voltages. As the Arrhenius plots appear to exhibit

a thermally activated behaviour, it is reasonable to assume that the reverse current can be expressed as [21]

$$J_R(T) = \alpha \exp\left(-\frac{E_r}{k_B T}\right) \tag{7}$$

where E_r is the activation energy. The calculated values of E_r for the three junctions are tabulated in Table 2.

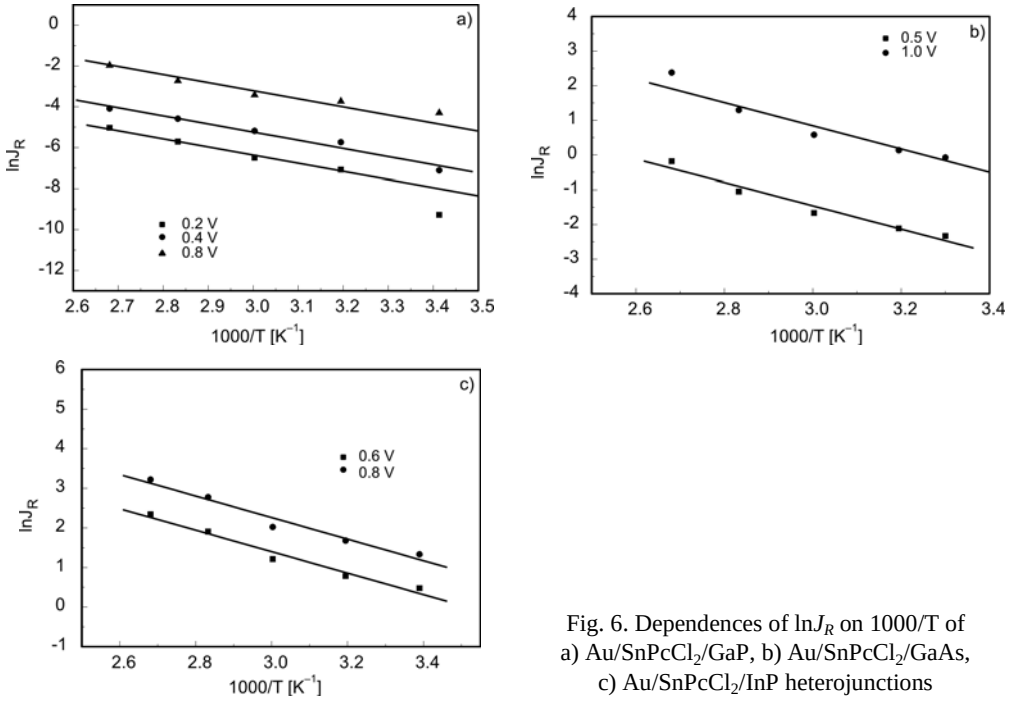

Fig. 6. Dependences of $\ln J_R$ on 1000/T of a) Au/$SnPcCl_2$/GaP, b) Au/$SnPcCl_2$/GaAs, c) Au/$SnPcCl_2$/InP heterojunctions

3.2. Capacitance–voltage characteristics

The capacitance of the heterojunctions (Au/$SnPcCl_2$/GaP, Au/$SnPcCl_2$/GaAs and Au/$SnPcCl_2$/InP) were measured at 1 MHz and at various temperatures. Figure 7 shows the dependence of $1/C^2$ with the voltage across the junctions. It is clear from the figure that the capacitances of the samples increase with the increase in temperature. Also, the values of C^{-2} on V varies linearly with the applied voltage, indicating that the junctions have an abrupt nature and the voltage dependence is [22]:

$$C^{-2} = \frac{2(V_d - V)(\varepsilon_1 N_1 + \varepsilon_2 N_2)}{qA^2 \varepsilon_0 \varepsilon_1 \varepsilon_2 N_1 N_2} \tag{8}$$

where V_d is the built-in voltage, ε_i is the electric permittivity and N_i is the donor (or acceptor) concentration; $i = 1$ or 2 denotes the two semiconductors that form the junction.

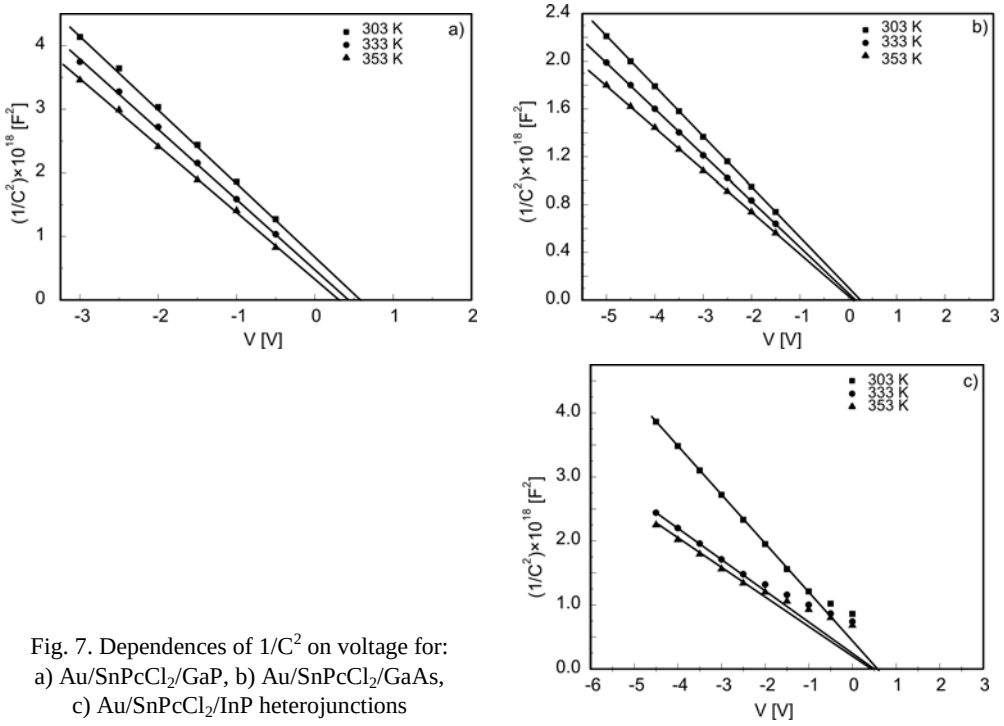

Fig. 7. Dependences of $1/C^2$ on voltage for: a) Au/SnPcCl$_2$/GaP, b) Au/SnPcCl$_2$/GaAs, c) Au/SnPcCl$_2$/InP heterojunctions

Table 3. Electrical parameters calculated from the *C–V* measurements for SnPcCl$_2$/GaP, SnPcCl$_2$/InP and SnPcCl$_2$/GaAs devices

Heterojunction	Temperature					
	303 K		333 K		353 K	
	Parameter					
	V_d [V]	N [m^{-3}]	V_d [V]	N [m^{-3}]	V_d [V]	N [m^{-3}]
SnPcCl$_2$/GaP	0.58	7.33×10^{20}	0.42	7.74×10^{20}	0.30	8.07×10^{20}
SnPcCl$_2$/InP	0.55	5.52×10^{19}	0.50	8.13×10^{19}	0.46	9.59×10^{19}
SnPcCl$_2$/GaAs	0.25	9.12×10^{20}	0.15	9.92×10^{20}	0.09	1.08×10^{21}

Equation (8) can be reduced to [23]:

$$C^{-2} = \frac{2(V_d - V)}{q\varepsilon_0 \varepsilon N A^2} \tag{9}$$

where ε is the electric permittivity of SnPcCl$_2$, A is the effective area of the device and N is the free carrier concentration. The built-in voltages of the junctions were calcu-

lated by extrapolating the $1/C^2$ curve to $V = 0$ and from the slope of the straight lines the values of N can be determined. The calculated values of V_d and N are compiled in Table 3. It can be seen from these tables that the built-in voltage decreases with the increase in temperature, while the carrier concentration increases with the increase in temperature.

4. Conclusion

The electrical characteristics of OI semiconductor diodes $SnPcCl_2$/GaP, $SnPcCl_2$/GaAs and $SnPcCl_2$/InP have been studied. Thermionic emission conduction in the low voltage range has been identified from the forward bias current density –voltage (J–V) measurements at various temperatures for the three devices. The contact barrier height for the $SnPcCl_2$/GaP heterojunction device is larger than those obtained for the $SnPcCl_2$/GaAs and $SnPcCl_2$/InP devices. At higher voltages, a space charge limited current (SCLC) controlled by an exponential trapping distribution above the valence band edge has been observed. Some electrical parameters, derived from the J–V analysis in the SCLC region, are consistent with the values reported for some other metal phthalocyanines. The C–V measurements showed that the heterojunctions have an abrupt nature. The built-in potential V_d decreases with the increase in temperature, while the carrier concentration N increases with the increase in temperature.

References

[1] VEAREY-ROBERTS A.R., EVANS D.A., Appl. Phys. Lett., 86 (2005), 072105.
[2] SO F.F., FORREST S.R., J. Appl. Phys., 63 (1988), 442.
[3] ABDEL-MALIK T.G., ABDEL-LATIF R.M., Thin Solid Films, 305 (1997), 336.
[4] GOULD R.D., SHAFAI T.S., Superfic., 9 (1999), 226.
[5] SAMUEL M., MENON C. S., UNNIKRISHNAN N. V., Mater. Sci.-Poland, 25 (2007), 177.
[6] PEUMANS P., BULOVIC V., FORREST S.R., Appl. Phys. Lett., 76 (2000), 2650.
[7] ZHOU X., PFEIFFER M., BLOCHWITZ J., WERNER A., NOLLAU A., FRITZ T., LEO K., Appl. Phys. Lett., 78 (2001), 410.
[8] NEWTON M.I., STARKE T.K.H., WILLIS M.R., MCHALE G., Sensors Act. B, 67 (2000), 307.
[9] KWONG C.Y., DJURISIC A.B., CHUI P.C., LAM L.S.M., CHAN W.K., Appl. Phys. A, 77 (2003), 555.
[10] PEISERT H., SCHWEIGER T., KNUPFER M., GOLDEN M.S., FINK J., J. Appl. Phys., 88 (2000), 1535.
[11] RIAD A.S., Thin Solid Films, 370 (2000), 253.
[12] TAKADA J., AWAJI H., KOSHIOKA M., NEVIN W.A., J. Appl. Phys., 75 (1994), 4055.
[13] LEE H.Y., KANG Y.S., JANG M.S., TANAKA H., KAWAI T., J. Korean Phys. Soc., 37 (2000), 475.
[14] MORGAN D.V., ALIYU Y., BUNCE R.W., Phys. Stat. Sol. (a), 133 (1992), 77.
[15] SHARMA G.D., SANGODKAR S.G., ROY M.S., Mat. Sci. Eng. B, 41 (1996), 222.
[16] FORREST S.R., KAPLAN M.L., SCHMIDT P.H., J. Appl. Phys., 60 (1986), 2406.
[17] SHARMA G.D., GUPTA S.K., ROY M.S., Thin Solids Films, 333 (1998), 176.

[18] EL-NAHASS M.M., ABD-EL-RMAN K.F., AL-GHAMDI A.A., ASIRI A.M., Physica B, 344 (2004), 398.
[19] GOULD R.D., J. Phys. D, 9 (1986), 1785.
[20] BAYHAN H., OZDEN S., Turk. J. Phys., 29 (2005), 371.
[21] CZERWINSKI A., SIMOEN E., POYAI A., CLAEYS C., J. Appl. Phys., 94, (2003), 1218.
[22] RIAD A.S., DARWISH S., AFIFY H.H., Thin Solid Films, 391 (2001), 109.
[23] DARWISH S., EL ZAWAWI I.K., RIAD A.S., Thin Solid Films, 485 (2005), 182.

Received 23 June 2008
Revised 3 November 2008